MINISTRY OF INDUSTRY AND TRADE
HANOI UNIVERSITY OF INDUSTRY

LE DUY LONG

RESEARCH ON THE EFFECTS OF BUS VIBRATIONS ON SEATED PASSENGERS

Major: Mechanical Engineering

Code: 9520116

SUMMARY OF DOCTORAL THESIS IN ENGINEERING

Hanoi - 2026

The project was completed at:
HANOI UNIVERSITY OF INDUSTRY – MINISTRY OF INDUSTRY AND TRADE

Scientific instructor:

1. **Associate Professor, Dr. Nguyen Thanh Quang**
2. **Associate Professor, Dr. Le Hong Quan**

Objection 1: Professor, Dr. Vu Duc Lap

Objection 2: Associate Professor, Dr. Dam Hoang Phuc

Objection 3: Associate Professor, Dr. Nguyen Tuan Nghia

The thesis was defended at the University-level Doctoral Thesis Evaluation Council and met at Hanoi University of Industry at 8 o'clock, date 29 month 1 year 2026.

The thesis can be found at:

- Hanoi University of Industry Library
- National Library of Vietnam

INTRODUCTION

Cars moving on the road when participating in traffic often generate vibrations. These vibrations will affect the driver and passengers in the car . Research on car vibrations shows that its impact has a great impact on human health such as neurological and brain diseases . If the vibration of the car is beyond the allowable range, it will affect the psychology, causing a bad state for the driver and passengers in the car , which can lead to dangers when participating in traffic.

1. Objective of the thesis

The objective of the dissertation is to conduct research on an actual passenger bus, using both theoretical analysis and experimental methods to investigate the effects of vehicle vibrations on passengers under the influences of road surface conditions and specific operating conditions. Based on the obtained results, the study provides a foundation for proposing passenger bus seats to be manufactured and assembled in Vietnam.

2. Research subjects

Choosing the 29-seat passenger van manufactured and assembled domestically is a representative vehicle type because it is widely used, accounts for a large proportion and is popular in Vietnam.

3. Scope of research

The thesis focuses on building and analyzing the spatial oscillation model of the vehicle affecting the occupants. The oscillation system of the vehicle - seat - occupant only considers the oscillation in the vertical direction (OZ axis), not considering the influence of the longitudinal and transverse directions (OX, OY).

Within the scope of the thesis, the thesis mainly evaluates the smoothness of vehicle motion and passenger comfort. The indicators related to vehicle motion safety or control stability are not within the scope of this study .

4. Research content

+ Establish a spatial model to survey the vibration of bus vehicles operating on the road surface close to reality to determine the displacement, velocity and acceleration values at the seat installation positions on the floor of the car to get input signals to affect the vibration model of the seat - the person sitting on the

seat. Different types of road surfaces include: sinusoidal, pulsed road surfaces, random road surface types and according to ISO 8608 standard used

+ Set up a chair-person oscillation model to determine the oscillation acceleration values at the chair and the body parts of the person sitting on the chair.

+ Conduct experiments to verify the model.

+ Compare with the standard for assessing the impact of vehicle vibration on vehicle occupants. The assessment criteria in the standard are calculated according to the RMS mean square value in the ISO 2631-1 standard.

5. Research methods

+ Theoretical research method: Build a model of a bus vehicle close to a real car. Use the Lagrange equation of the second type to establish models to survey the spatial vibration of the bus vehicle and the model of the person sitting on the seat. Use simulation software with external impacts: Road surface profile according to standards , specific speed ranges to solve and receive evaluation results . Price varies by vehicle and passengers.

+ Experimental research method: Conduct actual measurement experiments on traffic roads under conditions equivalent to the survey to measure the vibration parameters of Vehicle - Seat - Occupant.

6. Scientific and practical significance

Research on the application of modeling and simulation methods using spatial dynamics, using specialized software Matlab Simulink and Ansys Workbench, determine parameters affecting vehicle occupants, evaluating vehicle vibrations with experimental verification to propose solutions to improve the quality of vehicle and vehicle occupants' smoothness.

Develop theoretical and experimental research methods. The research results allow to propose some solutions to reduce oscillations during design, gradually perfecting the research methodology for designing car body shells in a modern direction like the advanced countries are using.

7. New points of the thesis

Building a survey model of Vehicle - Seat - Occupant oscillation.

Combining the Seat-Occupant Oscillation Survey Model and the Survey Model spatial fluctuations of 29-seat passenger van .

Using a combination of specialized software Matlab Simulink and Ansys Workbench in simulation.

Develop an experimental research method to determine the effects of different road surface profiles and different operating conditions at different vehicle speeds.

8. Thesis layout

The thesis is presented in a structure of 04 chapters:

Chapter 1: Overview of the research on vibration

Chapter 2: Building a model to survey the vibration of the vehicle - seat - occupant system

Chapter 3: Survey of the effects of vibration on vehicle occupants

Chapter 4: Experimental research

General conclusion and further research directions of the thesis

CHAPTER 1 OVERVIEW OF THE RESEARCH ON VIBRATION

Chapter 1 focuses on research related to:

Identify the different sources of vehicle vibration: that is, engine imbalance during engine start-up, imbalance of rotating parts in the transmission system, road surface unevenness etc.

Research situation in the country and abroad in the field of automobile vibration and passenger vibration.

Identify three mechanical models: Mass-spring damper model, multi-body dynamic model, finite element model, in studying vehicle-seat-occupant oscillation.

From that drawing the following conclusions:

Chapter 1 of the thesis has determined the research objective is to survey and evaluate the external impacts: Road surface profile, speed factors on the smoothness of vehicle movement and occupants. To achieve this objective, the thesis has combined theoretical, simulation and experimental methods.

Theoretical research method: A mass–spring–damper model is selected, and the Lagrange equations of the second kind are applied to describe the vibration dynamics in space of the passenger bus and the passenger seated in the vehicle.

Experimental research method: Field measurements are conducted, and the obtained results are compared in order to evaluate the accuracy of the theoretical model.

The research review shows that studies on vehicle vibrations and the response of seated passengers mainly use multi-body dynamic models and finite element methods. However, due to the complexity of the human body and the interaction between the vehicle, seat, and passenger, evaluating the vibration behavior of the system still presents many challenges.

Through analyzing the research situation at home and abroad, the researcher has determined the research direction of the thesis : Determining the impact of vehicle vibration on people sitting in the vehicle, the research object is a 29-seat bus vehicle manufactured and assembled in Vietnam.

From studying the effects of vehicle vibrations on people sitting in the car, it is possible to give scientific opinions to contribute to manufacturers and users to improve the smoothness of the car and passengers sitting in the car .

CHAPTER 2: BUILDING A MODEL TO SURVEY THE VIBRATION OF THE VEHICLE - SEAT - OCCUPANT SYSTEM

Some of the contents researched and presented in chapter 2:

2.1 RESEARCH OBJECTS

The 29-seat County passenger van manufactured and assembled in Vietnam meets the requirements of the problem, figure 2.1.

Figure 2.11 County 29-seat passenger van

It has 28 passenger seats and 1 driver seat. Two representative passenger seats were selected for the survey: the passenger seat and the third row seat.

2.2 SURVEY MODEL OF VEHICLE - SEAT - OCCUPANT SYSTEM VIBRATION

2.2.1 Assumptions of the model

2.2.2 Modeling of oscillation systems

The road-vehicle-seat-occupant research model considering the two auxiliary seat positions and the third row seat is a 9-degree-of-freedom mechanical system with geometric parameters, dimensional coordinates and characteristic symbols described in Figure 2.3.

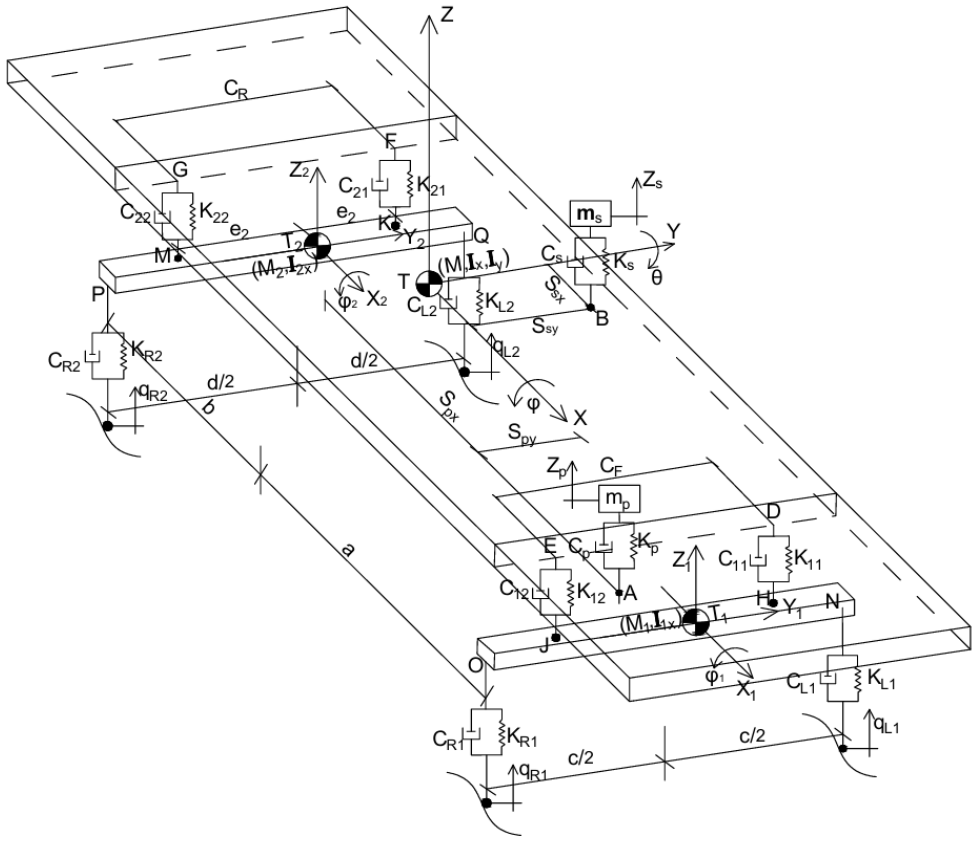

Figure 2.32 Vibration model of bus vehicle considering two seating positions

The degrees of freedom that determine the generalized coordinates of the system include:

Body: 3 degrees of freedom are vertical displacement Z and 2 longitudinal roll angles φ_x , shake sideways φ_y

Front axle: 2 degrees of freedom are vertical displacement and rotation angle along the OX axis, the generalized coordinates are z_{1z}, φ_{1x}.

Rear axle: 2 degrees of freedom are vertical displacement and rotation angle along the longitudinal axis OX coordinates z_{2z}, φ_{2x}.

The passenger seat (Z_p) has mass m_p and linear elastic elements with stiffness coefficient K_p and damping coefficient C_p.

The third row seat (Z_s) has mass m_s and linear elastic elements with stiffness coefficient K_s and damping coefficient C_s.

2.2.3 Construct the differential oscillation equation of the system

1. Equation for the generalized coordinate z (vertical displacement of the vehicle body)

$$\begin{aligned}&M\ddot{z} + (C_{11} + C_{12} + C_{21} + C_{22})\dot{z} - (C_{11} + C_{12})\dot{z}_{1z} - (C_{21} + C_{22})\dot{z}_{2z} + \\&(aC_{11} + aC_{12} - bC_{21} - bC_{22})\dot{\varphi}_x + (-cC_{11} + cC_{12} - dC_{21} + dC_{22})\dot{\varphi}_y - \\&(cC_{11} - cC_{12})\dot{\varphi}_{1x} - (dC_{21} - dC_{22})\dot{\varphi}_{2x} - C_p(\dot{z}_p - \dot{z} - S_{px}\dot{\varphi}_x - S_{py}\dot{\varphi}_y) - \\&C_s(\dot{z}_s - \dot{z} - S_{px}\dot{\varphi}_x - S_{py}\dot{\varphi}_y) + (K_{11} + K_{12} + K_{21} + K_{22})z - (K_{11} + K_{12})z_{1z} - \\&(K_{21} + K_{22})z_{2z} + (aK_{11} + aK_{12} - bK_{21} - bK_{22})\varphi_x + (-cK_{11} + cK_{12} - dK_{21} + \\&dK_{22})\varphi_y - (cK_{11} - cK_{12})\varphi_{1x} - (dK_{21} - dK_{22})\varphi_{2x} - K_p(z_p - z - S_{px}\varphi_x - \\&S_{py}\varphi_y) - K_s(z_s - z - S_{px}\varphi_x - S_{py}\varphi_y) = 0\end{aligned} \quad (2.22)$$

2. Equation for the generalized coordinate φ_x (longitudinal yaw angle of the vehicle body)

$$\begin{aligned}&I_X\ddot{\varphi}_x + (a^2C_{11} + a^2C_{12} + b^2C_{21} + b^2C_{22})\dot{\varphi}_x + (aC_{11} + aC_{12})\dot{z} - (aC_{11} + aC_{12})\dot{z}_{1z} - \\&(-bC_{21} - cC_{22})\dot{z}_{2z} + (-acC_{11} + acC_{12} + bdC_{21} - bdC_{22})\dot{\varphi}_y - (acC_{11} - acC_{12})\dot{\varphi}_{1x} - \\&(bdC_{21} - bdC_{22})\dot{\varphi}_{2x} - S_{px}C_p(\dot{z}_p - \dot{z} - S_{px}\dot{\varphi}_x - S_{py}\dot{\varphi}_y) - S_{sx}C_s(\dot{z}_s - \dot{z} - S_{sx}\dot{\varphi}_x - \\&S_{sy}\dot{\varphi}_y) + (a^2K_{11} + a^2K_{12} + b^2K_{21} + b^2K_{22})\varphi_x - (aK_{11} + aK_{12})(z - z_{1z}) - \\&(bK_{21} + bK_{22})(z - z_{2z}) + (-acK_{11} + acK_{12} + bdK_{21} - bdK_{22})\varphi_y - (-acK_{11} - \\&acK_{12})\varphi_{1x} - (bdK_{21} - bdK_{22})\varphi_{2x} - S_{px}K_p(z_p - z - S_{px}\varphi_x - S_{py}\varphi_y) - \\&S_{sx}K_s(z_s - z - S_{sx}\varphi_x - S_{sy}\varphi_y) = 0\end{aligned} \quad (2.23)$$

3. Equation for the generalized coordinate φ_y (side roll angle of the vehicle body)

$$\begin{aligned}&I_y\ddot{\varphi}_y + (c^2C_{11} + c^2C_{12} + d^2C_{21} + d^2C_{22})\dot{\varphi}_y + (-cC_{11} + cC_{12})\dot{z} - (-cC_{11} + cC_{12})\dot{z}_{1z} - \\&(-dC_{21} + dC_{22})\dot{z}_{2z} + (-acC_{11} + acC_{12} + bdC_{21} - bdC_{22})\dot{\varphi}_x - (c^2C_{11} + c^2C_{12})\dot{\varphi}_{1x} - \\&(d^2C_{21} + d^2C_{22})\dot{\varphi}_{2x} - S_{py}C_p(\dot{z}_p - \dot{z} - S_{px}\dot{\varphi}_x - S_{py}\dot{\varphi}_y) - S_{sy}C_s(\dot{z}_s - \dot{z} - S_{sx}\dot{\varphi}_x - \\&S_{sy}\dot{\varphi}_y) + (c^2K_{11} + c^2K_{12} + d^2K_{21} + d^2K_{22})\varphi_y + (-cK_{11} + cK_{12})(z - z_{1z}) - \\&(-dK_{21} + dK_{22})(z - z_{2z}) + (-acK_{11} + acK_{12} + bdK_{21} - bdK_{22})\varphi_x - (c^2K_{11} - \\&c^2K_{12})\varphi_{1x} - (d^2K_{21} - d^2K_{22})\varphi_{2x} - S_{py}K_p(z_p - z - S_{px}\varphi_x - S_{py}\varphi_y) - S_{sy}K_s(z_s - z - \\&S_{sx}\varphi_x - S_{sy}\varphi_y) = 0\end{aligned} \quad (2.24)$$

4. Equation for the generalized coordinate z_1 (vertical displacement of the front axle)

$$\begin{aligned}&m_1\ddot{z}_{1z} - (C_{11} + C_{12})(\dot{z} - \dot{z}_{1z}) - (aC_{11} + aC_{12})\dot{\varphi}_x - (-cC_{11} + cC_{12})\dot{\varphi}_y - \\&(-cC_{11} + cC_{12})\dot{\varphi}_{1x} + (K_{L1} + K_{R1})\dot{z}_{1z} - (K_{L1} - K_{R1})c\dot{\varphi}_{1x} - K_{L1}\dot{q}_{L1} - K_{R1}\dot{q}_{R1} - \\&(K_{11} + K_{12})(z - z_{1z}) - (aK_{11} + aK_{12})\varphi_x - (-cK_{11} + cK_{12})\varphi_y - (-cK_{11} + \\&cK_{12})\varphi_{1x} + (C_{L1} + C_{R1})z_{1z} - (C_{L1} - C_{R1})c\varphi_{1x} - C_{L1}q_{L1} - C_{R1}q_{R1} = 0\end{aligned} \quad (2.25)$$

5. Equation for the generalized coordinate φ_1 (roll angle of the front axle)

$$I_{1x}\ddot{\varphi}_{1x} - (cC_{11} - cC_{12})(\dot{z} - \dot{z}_{1z}) - (acC_{11} - acC_{12})\dot{\varphi}_x - (c^2C_{11} - c^2C_{12})\dot{\varphi}_y - (c^2C_{11} + c^2C_{12})\dot{\varphi}_{1x} - (K_{L1} - K_{R1})c\dot{z}_{1z} + (K_{L1} + K_{R1})c^2\dot{\varphi}_{1x} + K_{L1}c\dot{q}_{L1} - K_{R1}c\dot{q}_{R1} - (cK_{11} - cK_{12})(z - z_{2z}) - (acK_{11} - acK_{12})\varphi_x - (c^2K_{11} + c^2K_{12})\varphi_y - (c^2K_{11} + c^2K_{12})\varphi_{1x} - (C_{L1} - C_{R1})cz_{1z} + (C_{L1} + C_{R1})c^2\varphi_{1x} + C_{L1}cq_{L1} - C_{R1}cq_{R1} + C_F\varphi_{1x} = 0 \quad (2.26)$$

6. Equation for the generalized coordinates Z_{1X} (vertical displacement of the rear axle)

$$m_2\ddot{z}_{2z} - (C_{21} + C_{22})(\dot{z} - \dot{z}_{2z}) - (-bC_{21} - bC_{22})\dot{\varphi}_x - (-dC_{21} + dC_{22})\dot{\varphi}_y - (-dC_{21} + dC_{22})\dot{\varphi}_{2x} + (K_{L2} + K_{R2})\dot{z}_{2z} - (K_{L2} - K_{R2})d\dot{\varphi}_{2x} - K_{L2}\dot{q}_{L2} - K_{R2}\dot{q}_{R2} - (K_{21} + K_{22})(z - z_{2z}) - (-bK_{21} - bK_{22})\varphi_x - (-dK_{21} + dK_{22})\varphi_y - (-dK_{21} + dK_{22})\varphi_{2x} + (C_{L2} + C_{R2})z_{2z} - (C_{L2} - C_{R2})d\varphi_{2x} - C_{L2}q_{L2} - C_{R2}q_{R2} = 0 \quad (2.27)$$

7. Equation for the generalized coordinates φ_{2X} (roll angle of the rear axle)

$$I_{2x}\ddot{\varphi}_{2x} - (dC_{21} - dC_{22})(\dot{z} - \dot{z}_{2z}) - (bdC_{21} - bdC_{22})\dot{\varphi}_x - \left(d^2C_{21} - d^2C_{22}\right)\dot{\varphi}_y - \left(d^2C_{21} + d^2C_{22}\right)\dot{\varphi}_{2x} - (K_{L2} - K_{R2})d\dot{z}_{2z} + (K_{L2} + K_{R2})d^2\dot{\varphi}_{2x} + K_{L2}d\dot{q}_{L2} - K_{R2}d\dot{q}_{R2} - (dK_{21} - dK_{22})(z - z_{2z}) - (bdK_{21} - bdK_{22})\varphi_x - (d^2K_{21} - d^2K_{22})\varphi_y - (d^2K_{21} + d^2K_{22})\varphi_{2x} - (C_{L2} - C_{R2})dz_{2z} + (C_{L2} + C_{R2})d^2\varphi_{2x} + C_{L2}dq_{L2} - C_{R2}dq_{R2} + C_R\varphi_{2x} = 0 \quad (2.28)$$

8. Equation for the generalized coordinates z_p (vertical displacement of the passenger seat)

$$m_p\ddot{z}_p + C_p\left(\dot{z}_p - \dot{z} - S_{px}\dot{\varphi}_x - S_{py}\dot{\varphi}_y\right) + K_p\left(z_p - z - S_{px}\varphi_x - S_{py}\varphi_y\right) = 0 \quad (2.29)$$

9. Generalized coordinate equation z_s (vertical displacement of row 3 seats)

$$m_s\ddot{z}_s + C_s\left(\dot{z}_s - \dot{z} - S_{sx}\dot{\varphi}_x - S_{sy}\dot{\varphi}_y\right) + K_s\left(z_s - z - S_{sx}\varphi_x - S_{sy}\varphi_y\right) = 0 \quad (2.30)$$

The vehicle's oscillation equation system is written in matrix form.

$$[M]\{\ddot{q}\} + [C]\{\dot{q}\} + [K]\{q\} = \{F(t)\} \quad (2.31)$$

The system is affected by the coordinates of the vehicle's center of gravity, the position of the seat - the occupants appear to redistribute the load. At this time, F(t) will include two components: The excitation force from the road surface and the force due to the redistribution of the load.

2.3. BUILDING A MODEL OF VIBRATION OF AN OCCUPANT

The degrees of freedom of the system determine the vertical displacements of the blocks respectively include: Z_d : displacement of the head block; Z_n : displacement of the chest block; Z_m: displacement of the body block; Z_{gh} : displacement of the chair block (figure 2.4)

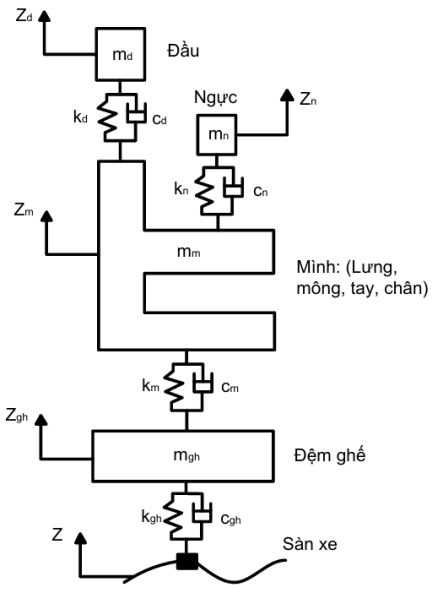

Figure 2.4 Oscillation model of passenger seat occupants.

Build the system of differential equations for oscillation of an occupant.

Applying Newton's equations II and III, considering the balance of the force system, the equations describing the oscillation of the system of a person sitting on a chair include 4 equations from (3.1) to (3.4)

$$m_{gh}\ddot{Z}_{gh} = k_{gh}(Z - Z_{gh}) + k_m(Z_m - Z_{gh}) + c_{gh}(\dot{Z} - \dot{Z}_{gh}) + c_m(\dot{Z}_m - \dot{Z}_{gh}) \quad (2.34)$$

$$m_m\ddot{Z}_m = k_m(Z_{gh} - Z_m) + k_n(Z_n - Z_m) + c_m(\dot{Z}_{gh} - \dot{Z}_m) + c_n(\dot{Z}_n - \dot{Z}_m) \quad (2.35)$$

$$m_n\ddot{Z}_n = k_n(Z_m - Z_n) + c_n(\dot{Z}_m - \dot{Z}_n) \quad (2.36)$$

$$m_d\ddot{Z}_d = k_d(Z_m - Z_d) + c_d(\dot{Z}_m - \dot{Z}_d) \quad (2.37)$$

2.4. METHODS AND CRITERIA FOR ASSESSING THE IMPACT OF VIBRATION ON OCCUPANTS

2.4.1 Perception method

2.4.2 Smoothness of motion index

2.5. DETERMINING MODEL PARAMETERS

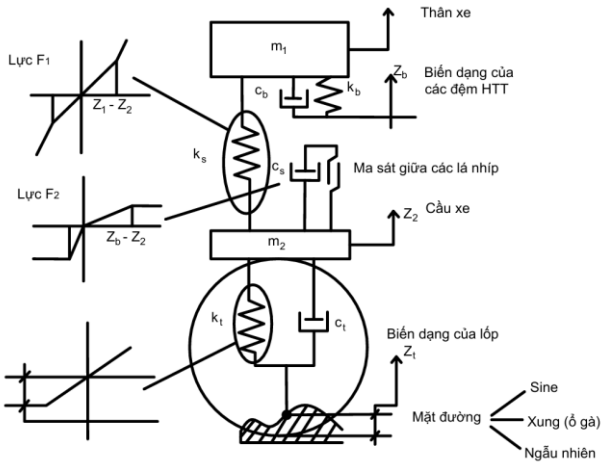

Figure 2.7 Oscillation diagram of vehicle suspension system

HTT hardness parameters include static hardness and dynamic hardness **.**

2.6 CONCLUSION OF CHAPTER 2

Based on the analysis, the County 29-seat passenger bus was selected as the research vehicle. This bus is assembled in Vietnam and widely used. Its technical and physical characteristics have been published in several previous studies, which can therefore be referenced and used in this dissertation.

Based on assumptions consistent with real operating conditions, a road–vehicle–seat–passenger vibration model was developed. The model is a 9-degree-of-freedom spatial vibration model, including 7 degrees of freedom of the vehicle and 2 degrees of freedom of the seat–passenger system. Two seat positions were selected for investigation: the assistant seat and the third-row seat, which allows the analysis to be extended to other seating positions throughout the vehicle.

Construct a system of 9 differential equations describing the vehicle's spatial oscillations to survey. The system of differential equations is written in the form of state equations with matrices A(18x18), B(18x4), C(9x9), D(9x4).

Building a dynamic model of the Seat - occupant system with 4 degrees of freedom including 1 degree of freedom of the seat and 3 degrees of freedom of the occupant, based on the anthropometric characteristics of Vietnamese people and selecting evaluation criteria according to ISO 2631-1 and QCVN 27/2016/BYT . The parameters of the suspension system, tires and seats are determined from design characteristics, published data and previous studies.

CHAPTER 3: SURVEY ON THE IMPACT OF VIBRATION ON VEHICLE OCCUPANTS

3.1. ROAD SURFACE STIMULATIONS ON THE MODEL

Establish the equation for the excitation force vector {F(t)}, independently examine 4 types of excitation: Sinusoidal bump, pulse bump, random bump, ISO 8608 type C bump.

These excitations are determined at four points of contact between the wheel and the road surface: q_{L_1} (front left), q_{L2} (rear left), q_{R1} (front right), and q_{R_2} (rear right).

3.2. SURVEY OF FLUCTUATIONS OF 29-SEAT PASSENGER BUS

The survey conditions include: Vehicle speeds of 20, 40, 60, 80, 100 km/h and four road surfaces: sinusoidal, pulsed, random and ISO 8608.

3.2.1 Displacement and acceleration of generalized coordinates

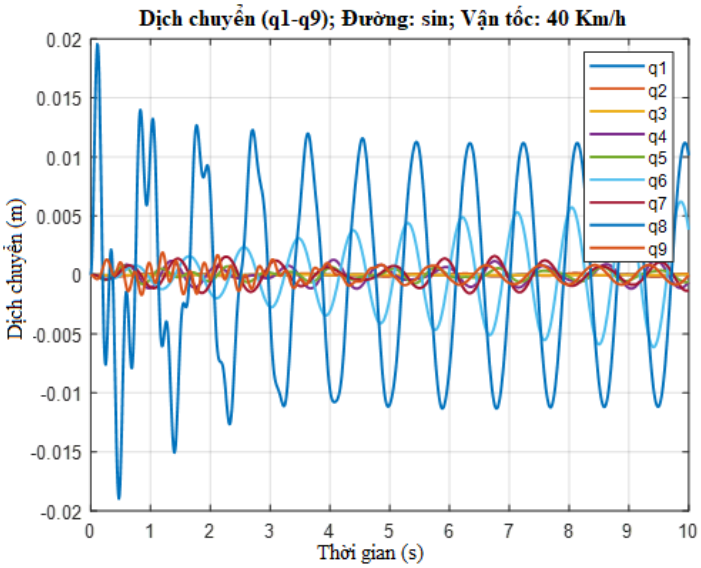

Figure 3.2 Vertical displacement amplitude of vehicle oscillation

Oscillation displacement amplitude. Observation on the graph shows that at the vehicle speed of 40 km/h, the bumpy road surface is sinusoidal, the displacement amplitude of the suspended mass q_1 is the largest, the peak value of the oscillation is approximately 20 mm, followed by the unsuspended mass q6. The passenger seat position q_8 and the third-row seat q_9 have relatively even and lower oscillation amplitudes, figure 3.2.

Acceleration of oscillation: At vehicle speed mode of 40 km/h, the road surface is sine-scale, the suspended mass q_1 has the largest oscillation acceleration, the peak value reaches 7 (m/s^2). Other generalized coordinates including q_8 , q_9 are approximately the same. All oscillations tend to gradually damp out due to the influence of damping, figure 3.3.

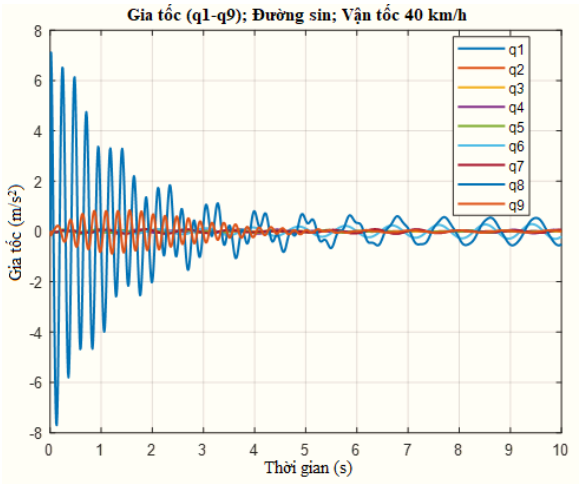

Figure 3.3 Oscillation acceleration on bus vehicle

Comparison of survey results shows that under different operating modes of vehicle speed, the type of road surface roughness clearly affects the amplitude and acceleration of oscillation.

3.2.2 Types of road surfaces

The unevenness of the road surface creates excitation forces on the four wheels, the frequency of the excitation force tends to increase with the increase in speed. Figure 3.4 shows the increasing trend of the amplitude of the excitation force on the four wheels.

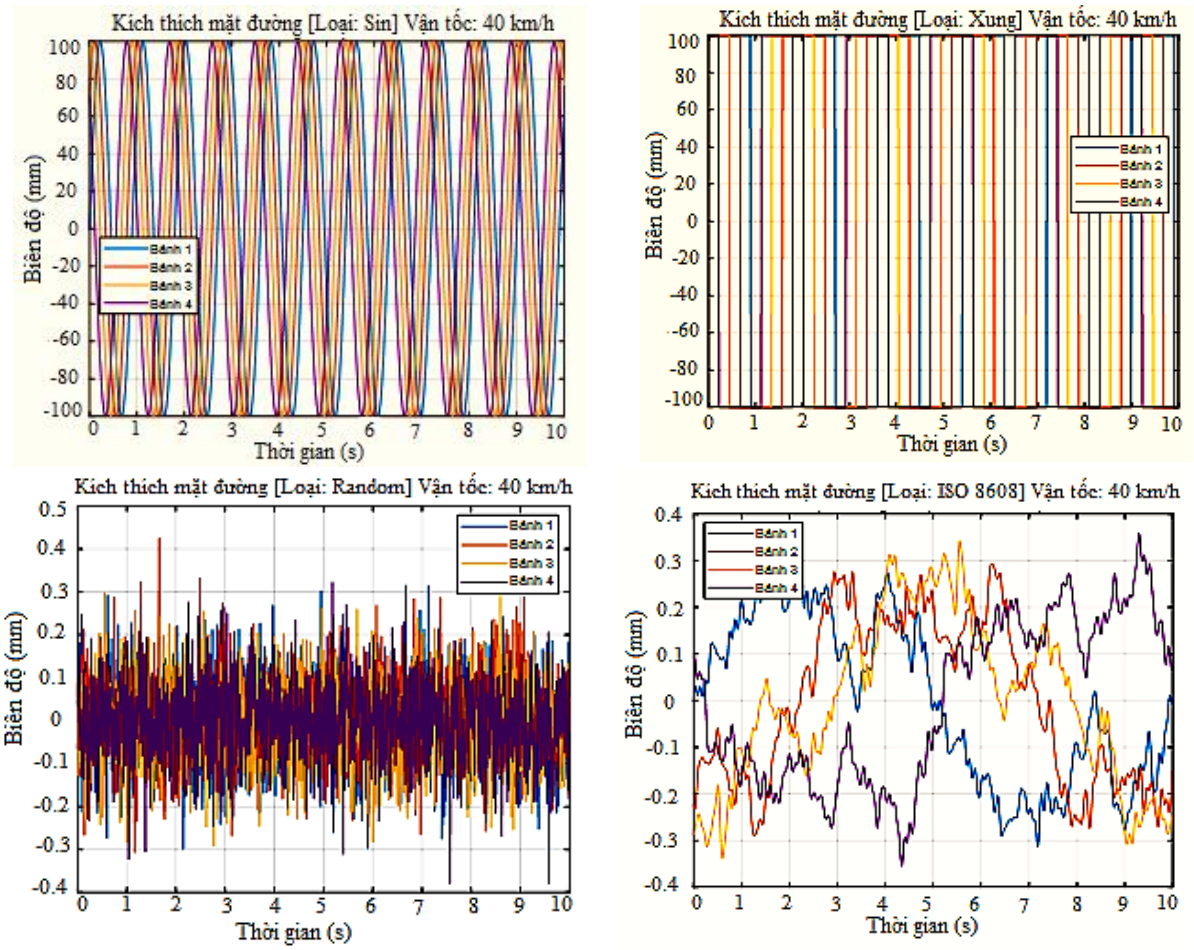

Figure 3.4 Sinusoidal, pulsed, random and ISO 8608 road surface excitation graphs

3. 2.3 Frequency response analysis

Figure 3.5 shows that the frequency response of the generalized coordinate systems q_1, q_2, q_3 is stable in the low frequency region. In the middle region, the average frequency has sudden spikes at the same time and gradually decreases in the higher frequency region.

The phasor diagram shows the phase shift of the output signal compared to the input signal with frequency to evaluate the delay or increase in phase at each frequency. Thus, in the middle region of the system, instability occurs.

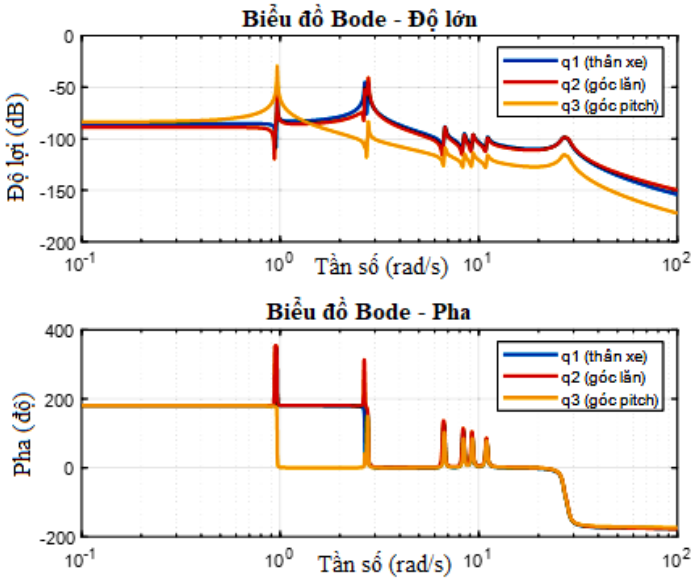

Figure 3.5 Frequency response graph of q_1, q_2, q_3.

3.1.4 Analysis of sitting position fluctuations

In the specific survey mode with a vehicle speed of 40 km/h, the sinusoidal road surface undulation shows that the passenger seat position has a larger oscillation amplitude than the passenger seat position in the third row. The evaluation of the oscillation acceleration is also consistent with the law of displacement, figure 3.6.

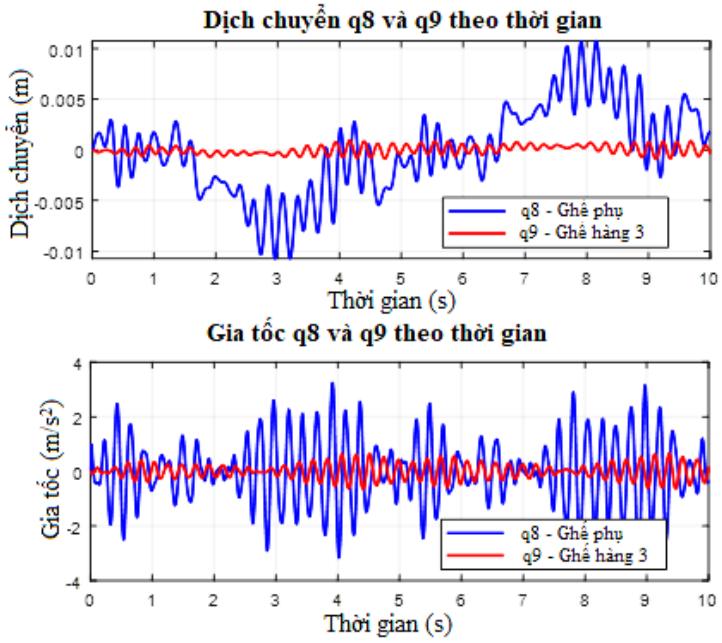

Figure 3.6 Oscillation graph of two generalized coordinates q_8, q_9

Frequency spectrum analysis shows that in the low frequency region the amplitude of high oscillation reaches a peak value, then decreases and stabilizes in the high frequency region, figure 3.7.

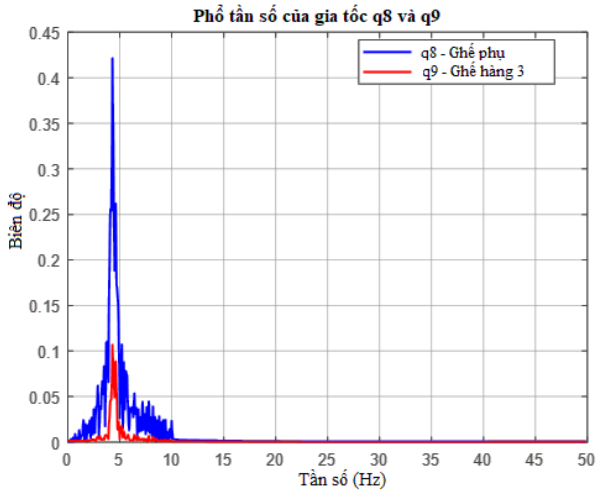

Figure 3.7 Frequency spectrum graph of acceleration q_8, q_9

3.3 SIMULATION OF PERSON SITTING ON A CHAIR

3.3.1 Stimulation signal to the chair

In figure 3.11 is the graph of the displacement results of the oscillation at the passenger seat at 5 vehicle speed ranges in the simulation that have been determined.

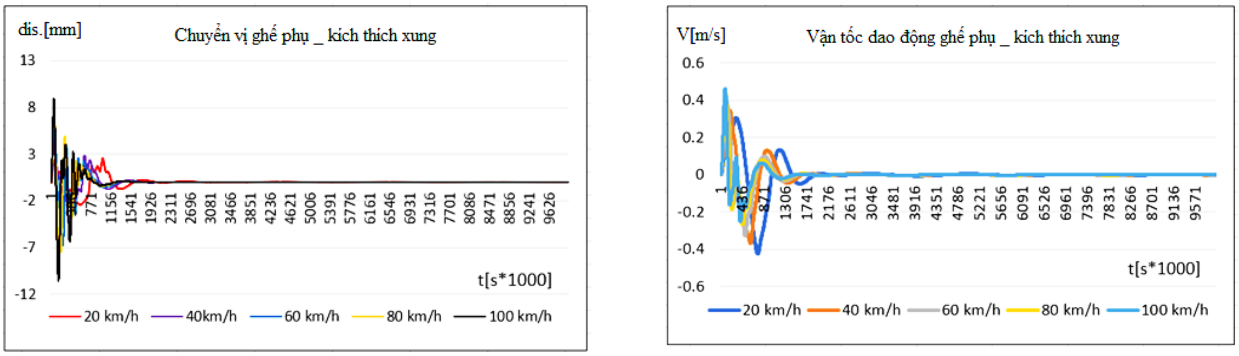

a) Move the passenger seat *b) Vibration velocity of the passenger seat*

Figure 3.11 Graph of excitation signal to passenger seat when vehicle passes over bumpy road

Compare a specific result of the car running on a bumpy road, speed of 40 km/h on the passenger seats, 3rd row seats to analyze the results. In figure 3.12.a,b are the displacement results at 2 corresponding seat positions.

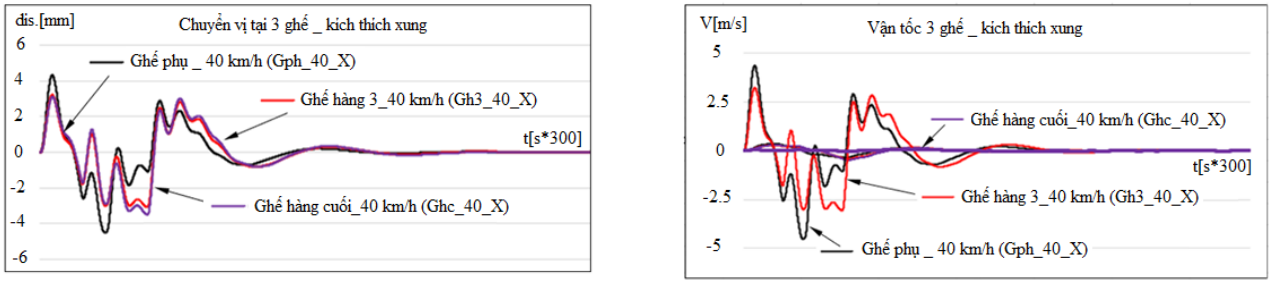

a) Transposition on 2 seat positions *b) Oscillation velocity of 2 seat positions*

Figure 3.12 Graph comparing displacement and oscillation velocity on 2 seat positions, vehicle speed 40 km/h

3.3.2 Simulation of vibration of an occupant

- Simulation of an occupant vibration on seat in sine and pulse waves, ISO 8608:

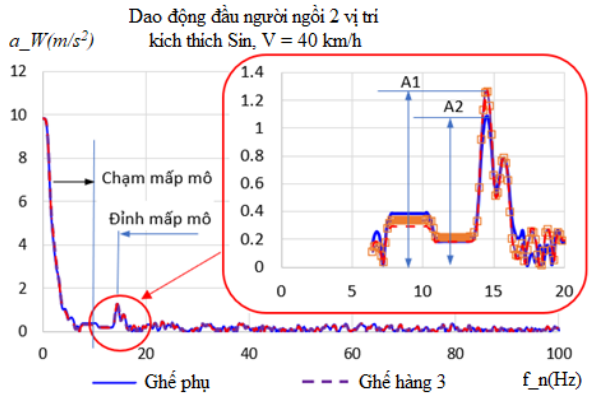

Figure 3.18 Oscillation graph in the frequency domain above the head at 2 seat positions, sine wave

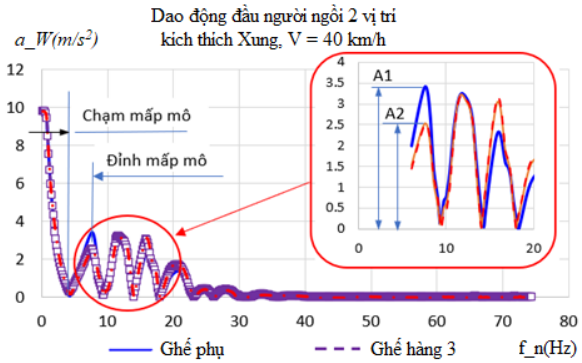

Figure 3.19 Frequency domain oscillation graphs above the head at two seat positions, bumpy PULSE

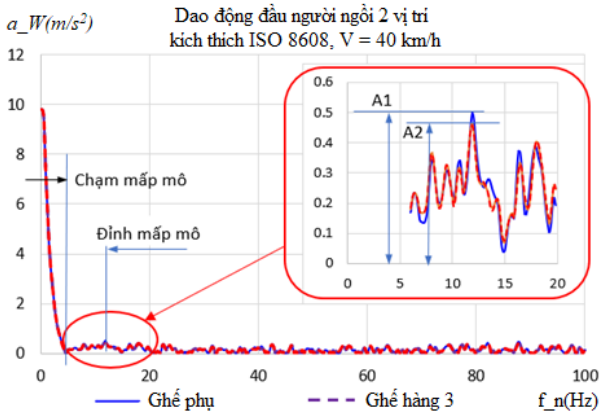

Figure 3.20 Frequency domain oscillation graphs above the head at two seat positions, ISO 8608 undulation

3.4 COMPARISON OF SIMULATION RESULTS

3.4.1 Comparison of head oscillation simulation results

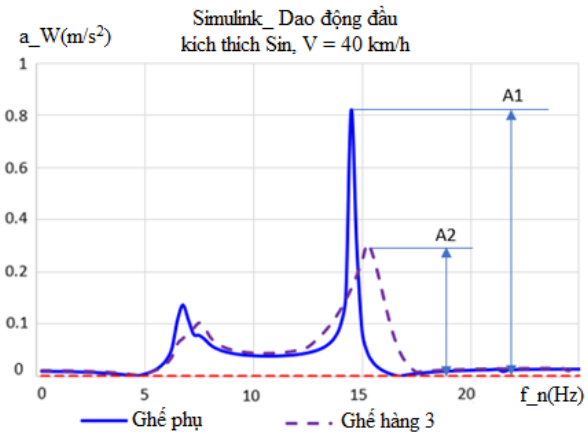

a) Results of Malab/Simulink simulation of human head oscillation

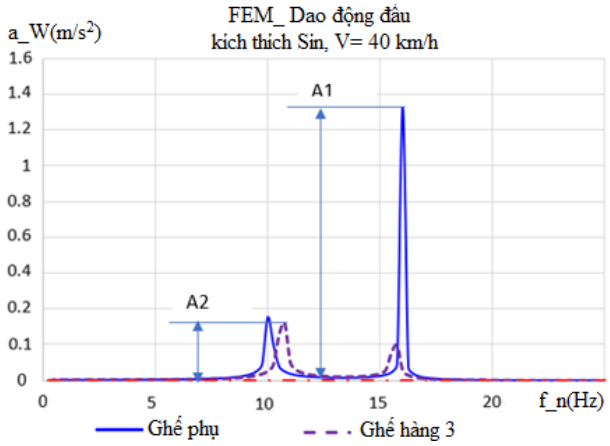

b) FEM/Ansys Workbench simulation results of human head oscillation

Figure 3.26 Simulation results of head oscillation of a person sitting on a chair

Person sitting in the passenger seat (A_1): in the Malab/Simulink simulation the head oscillation of the passenger seat has an acceleration of 0.82 (m/s^2) at a

frequency of 14 (Hz), the higher FEM simulation is 1.33 (m/s^2) at a higher frequency of 16 (Hz).

Person sitting on row 3 seat (A_2): in Malab/Simulink simulation the head oscillation of the person sitting on the passenger seat has an acceleration of 0.3 (m/s^2) at frequency 15.5 (Hz), the lower FEM simulation is 0.16 (m/s^2) at lower frequency 11 (Hz).

3.4.2 Comparison of chest oscillation simulation results

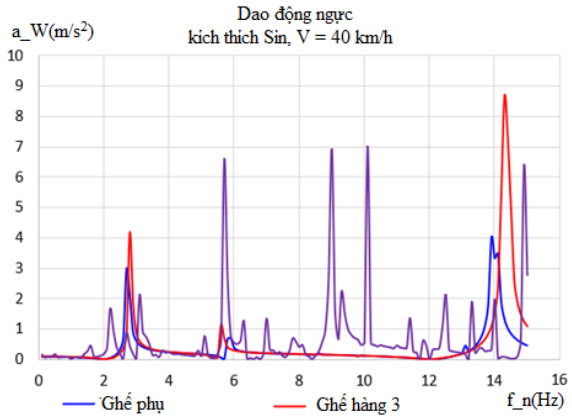

a) Malab/Simulink user chest oscillation simulation

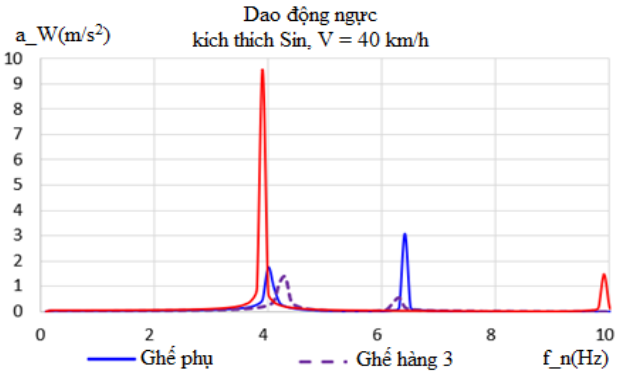

b) FEM/Ansys Workbench user simulated chest oscillation

Figure 3.27 Simulation results of chest vibration of a person sitting on a chair

Passenger seat occupant: in Malab/Simulink simulation the passenger seat occupant's chest oscillation has an acceleration of 4 (m/s^2) at a frequency of 14.2 (Hz), the lower FEM simulation is 3 (m/s^2) at a lower frequency of 6.5 (Hz).

Person sitting on row 3 seat: in Malab/Simulink simulation chest oscillation of person sitting on row 3 seat has acceleration 8.5 (m/s^2) at frequency 14.2 (Hz), lower FEM simulation is 1.5 (m/s^2) at lower frequency 4.2 (Hz).

3.4.3 Comparison of thigh oscillation simulation results

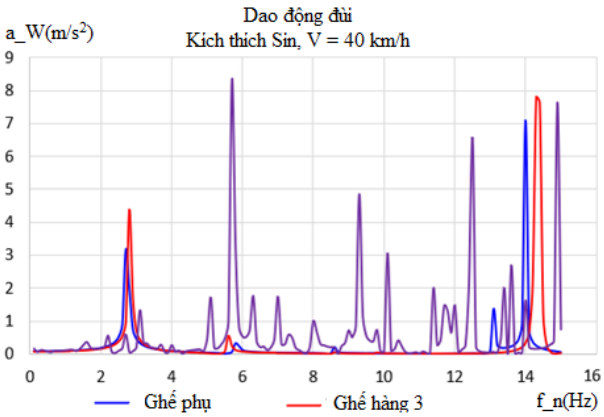

a) Malab/Simulink simulated human thigh oscillation

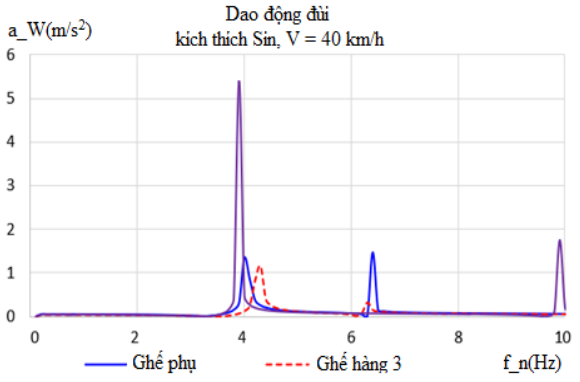

b) User thigh oscillation FEM/Ansys Workbench simulation

Figure 3.28 Simulation results of thigh oscillation of a person sitting on a chair

Passenger seat occupant: in Malab/Simulink simulation passenger seat occupant thigh oscillation has acceleration 7.1 (m/s^2) at frequency 14 (Hz), higher FEM simulation is 1.6 (m/s^2) at higher frequency 6.5 (Hz).

3rd row seat occupant: in Malab/Simulink simulation the passenger seat thigh oscillation has an acceleration of 7.9 (m/s^2) at a frequency of 14.2 (Hz), the lower FEM simulation is 1.1 (m/s^2) at a lower frequency of 4.1 (Hz).

3.4.4 Evaluation of simulation results

The comparison of the reliability value of the initial oscillation simulation method is shown in Figure 3.28 .

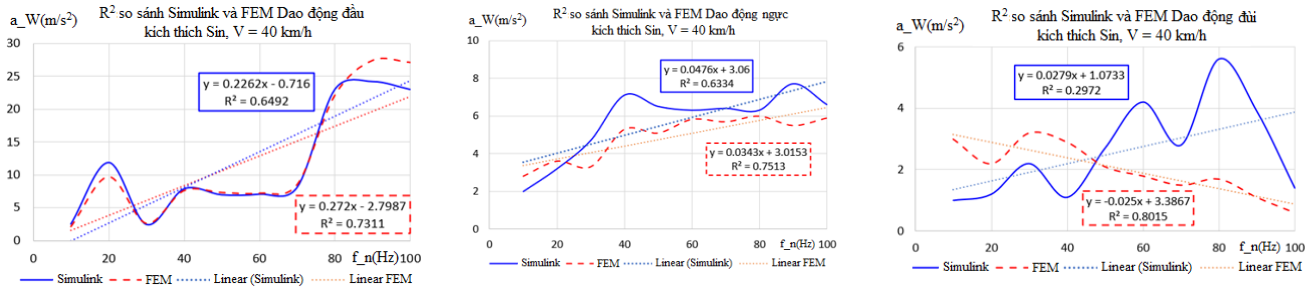

a) R ^{2} head oscillation *b) R ^{2} chest oscillation* *c) R ^{2} thigh oscillation*

Figure 3.29 Comparison graph of human vibration simulation methods

Comparing the regression equation and the R2 value ^{of} the square deviation of the fluctuations, we get quantitative data showing:

Simulink FEM simulation R ^{2} = 0.731 > 0.6429

Simulink FEM simulation R ^{2} = 0.7513 > 0.6334

Simulink FEM simulation R ^{2} = 0.8015 > 0.2972

Remarks: Finite element modeling (FEM) can be used as reference data for comparison with the simulation results obtained from Simulink, in order to validate the reliability of the simulation results.

3.5 ASSESSMENT OF THE IMPACT OF VIBRATION ON THE OCCUPANT

Frequency spectrum analysis in figure 3.31 of q_8 and q_9 shows:

- q_8 has a higher vibration amplitude in the low frequency region (below 5 Hz), reflecting the impact from the overall oscillation of the vehicle.

- q_9 has a higher amplitude at mid-frequency (~5-10 Hz), possibly due to the influence of seat suspension oscillation number 3.

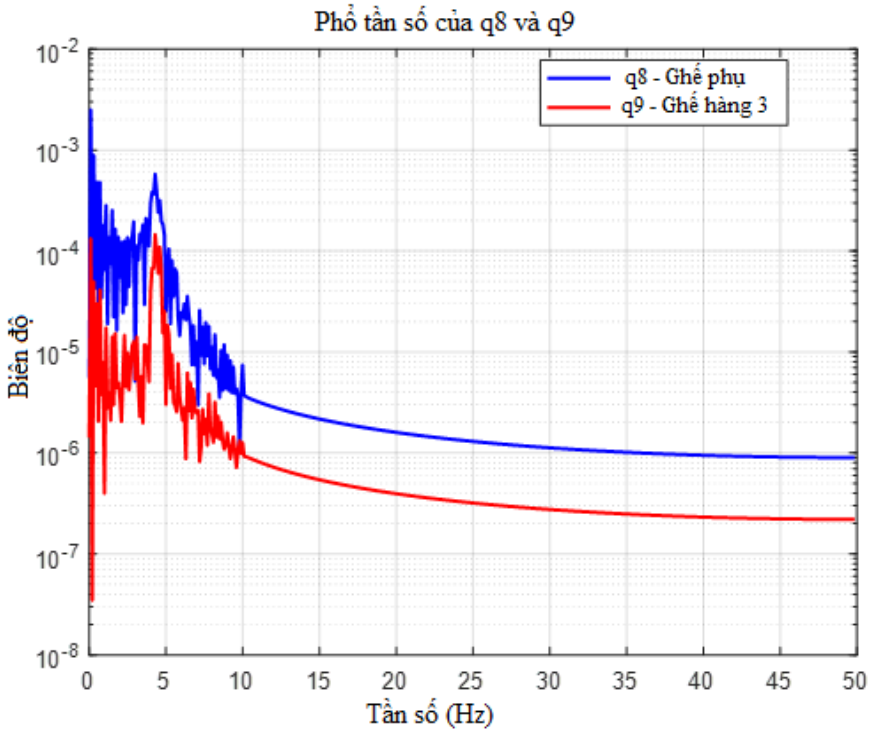

Figure 3.31 Frequency spectrum plot of q_8 and q_9

3.6 CONCLUSION OF CHAPTER 3

The vibration survey results show that the amplitude and acceleration of the vehicle vibration depend on the type of bump and the speed of movement. The time-domain and frequency-domain analyses indicate that the low-frequency region (1–10 Hz) has the strongest influence on the vibration transmitted to the occupants. At the same time, the passenger seat position is affected more than the third-row seat, especially in the case of pulse excitation. The vibration simulation results show that the values of displacement, velocity and acceleration of vibration are consistent with the theoretical basis of vibration in mechanics as well as the specialized field of automobile vibration.

The finite element method (FEM) was used to develop a 3D vibration model of the seat–passenger system that approximates real conditions as closely as possible. The simulation was performed using the specialized software Ansys Workbench, licensed version 2024 R2. The results were analyzed using the coefficient of determination (R^2), which indicates that the FEM results are reliable and can therefore be used for comparison with the simulation results obtained from Simulink.

A correlation matrix was developed and analyzed to determine the influence of vehicle vibrations on passengers. The results show that the research models presented in Chapters 2 and 3 are appropriate.

CHAPTER 4: EXPERIMENTAL RESEARCH

4.1 RESEARCH OBJECTIVES AND EXPERIMENTAL CONDITIONS

Compare with experimental results, evaluate the accuracy of the theoretical model and conclude the correctness of the research method.

Occupant vibration assessment according to ISO 2631 standard.

TEST SUBJECTS

The experimental subject is the 29-seat County passenger bus manufactured and assembled in Vietnam by Truong Hai Auto.

4.3 TEST LINE

The experiment for the vehicle to move on a road surface is a series of 3 road sections, the vehicle runs at different speed modes V=20 km/h, V= 40 km/h, V= 60 km/h.

+ The road section has random undulations, determined by direct measurement and tabulation of the average undulation values to determine the approximation compared to ISO 8608 type C standard.

+ The road section has a sinusoidal contour according to the basic standards of the Vietnam Road Administration, figure 4.2 .

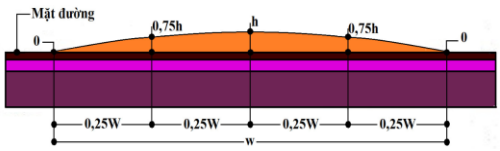

a. Standard sinusoidal contour line

b. Sine wave contour fabrication and installation on test track

Figure 4.2 Sinusoidal contour contour

+The road section has a bumpy contour according to the basic standards of the Vietnam Road Administration, figure 4.3.

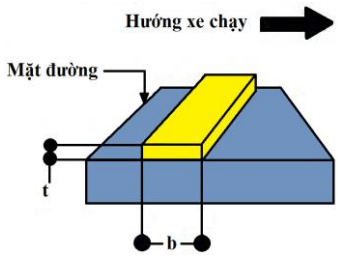

a. Bumpy pulse-shaped border, b = 200 mm; t = 60 mm

b. Pulse-shaped profile bumps are installed on the test track

Figure 4.3 Boundary surface undulation in the shape of a pulse

Test track location:

Figure 4.4 Test track location at Tay Tuu Street, Hanoi

4.4 LABORATORY EQUIPMENT

4.4.1 Dewesoft Sirius Mini 16 ACC and R2DB Data Collector

Figure 4.5 Dewesoft Sirius 16ACC and R2DB Data Collector

4.4.2 Accelerometer sensor ICP 356A16, Vibra-Metrics model 1001

Figure 4.6 3-axis acceleration ICP 356A16 sensor

Figure 4.7 Vibra-Metrics model 1001 accelerator sensor

4.4.3 DS-IMU1 velocity sensor , HF-750 displacement sensor

Figure 4.8 DS-IMU1 velocity sensor

Figure 4.9 HF-750 displacement sensor

4.5 SENSOR LAYOUT ON VEHICLE AND SENSOR DIAGRAM

4.5.1 Sensor installation layout plan

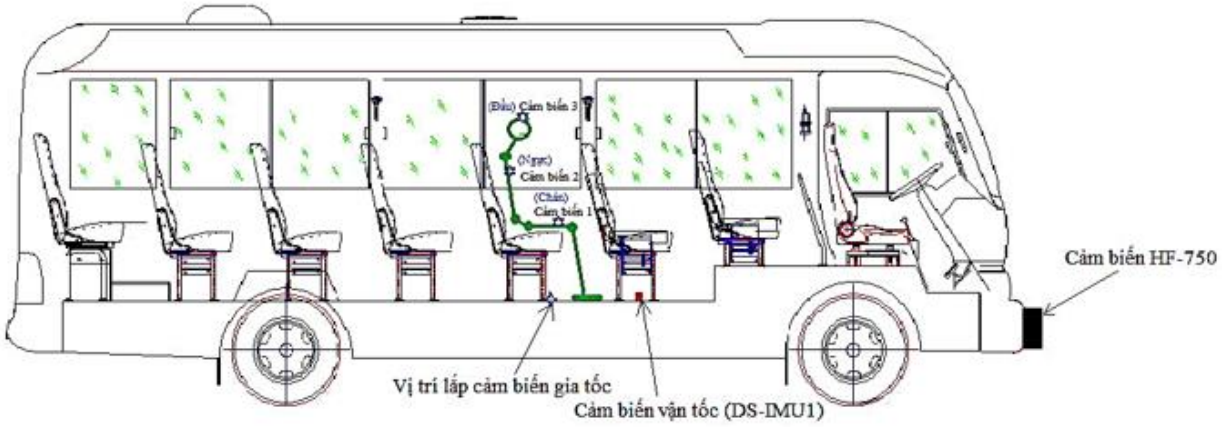

Figure 4.10 Schematic diagram of sensor installation on vehicles and people

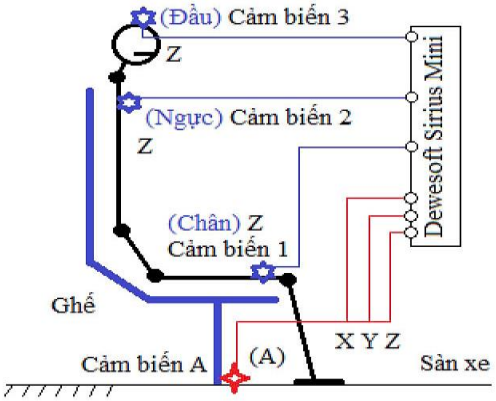

Figure 4.11 Diagram of measurement location on the body

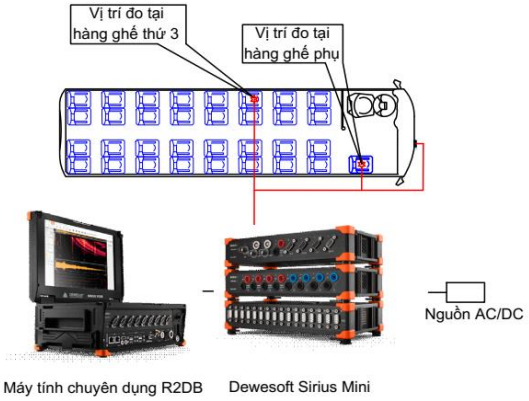

Figure 4.12 Diagram of measurement location on seat

4.5.2 Sensor connection diagram

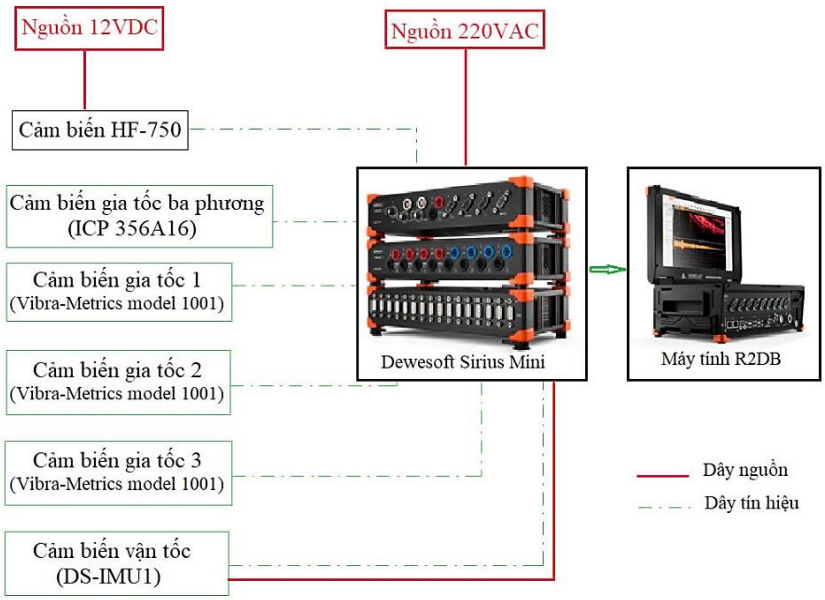

Figure 4.13 Sensor connection diagram

4.6 TEST MODES, INSTALLING SENSORS ON THE VEHICLE AND CONDUCTING EXPERIMENTS

Test modes	V = 20 (km/h)	V = 40 (km/h)	V = 60 (km/h)
File symbol	V20	V40	V60
Chair leg oscillation	A_20_XYZ	A_40_XYZ	A_60_XYZ
Human leg oscillation	CB1_20_Z	CB1_40_Z	CB1_60_Z
Human chest vibration	CB2_20_Z	CB2_40_Z	CB2_60_Z
Head oscillation	CB3_20_Z	CB3_40_Z	CB3_60_Z

4.7 COLLECTION AND PROCESSING OF EXPERIMENTAL DATA

4.7.1 Data collection

The results of experimental data collection in DewesoftX software are described in a case on the computer interface.

4.7.2 Analysis of experimental results

An illustrative form of the experimental results extracted is the RMS acceleration on the head, chest and thighs of a person sitting in a chair shown in Figure 4.24.a,b,c

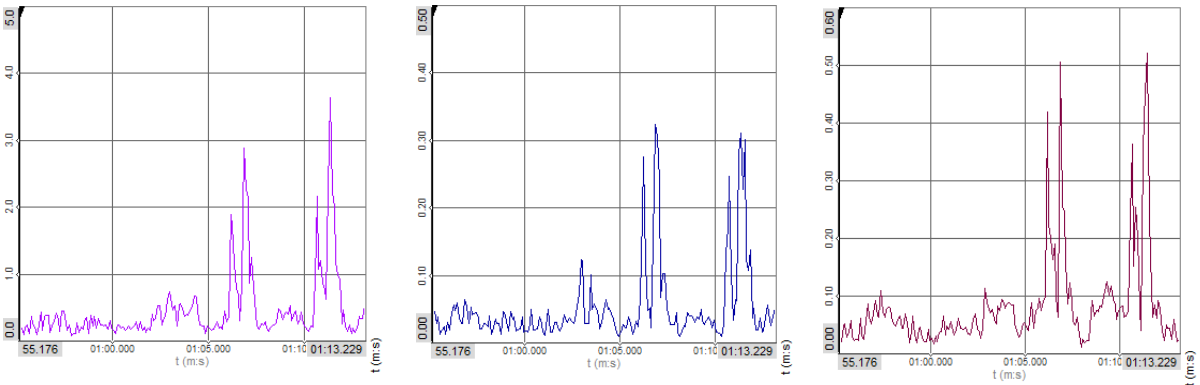

a. On the head *b. On the chest* *c. On the thigh*

Figure 4.24 RMS acceleration graph on body parts in Z direction of passenger seat, sinusoidal excitation, V = 40 km/h

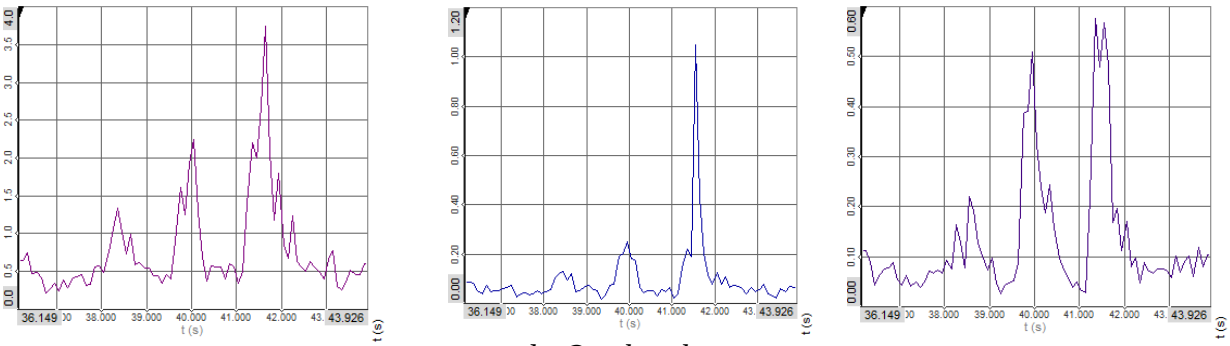

a. On the head *b. On the chest* *c. On the thigh*

Figure 4.25 RMS acceleration graph on body parts in Z direction of passenger seat, sinusoidal excitation, V = 60 km/h.

The experimental results give full results of RMS acceleration values of the two positions of the human body oscillation at other seat positions such as the passenger seat and the third row seat. The oscillation is mainly concentrated in the low frequency region, showing that the experimental results are consistent with the theory in Figure 4.24 and Figure 4.25.

The regression results between simulation and experiment are shown in the graphs of figure 4.31.a,b,c.

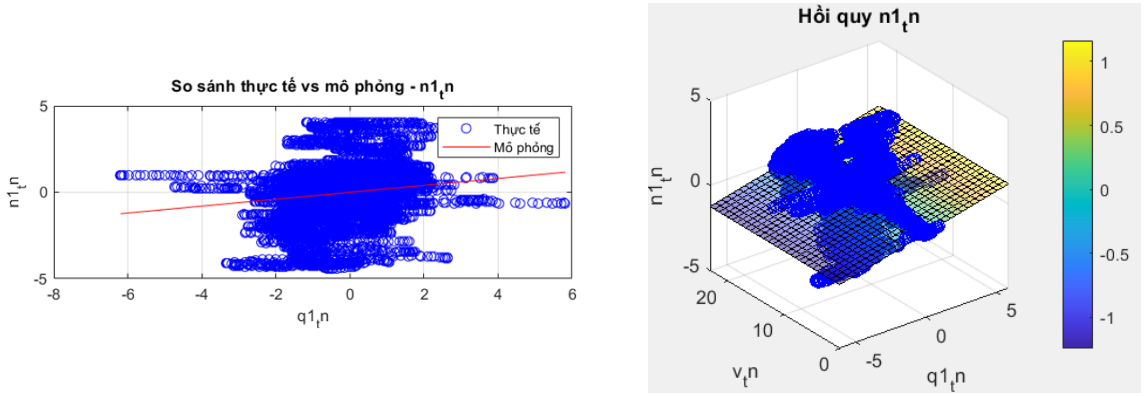

a) Regression between n 1 and q 1

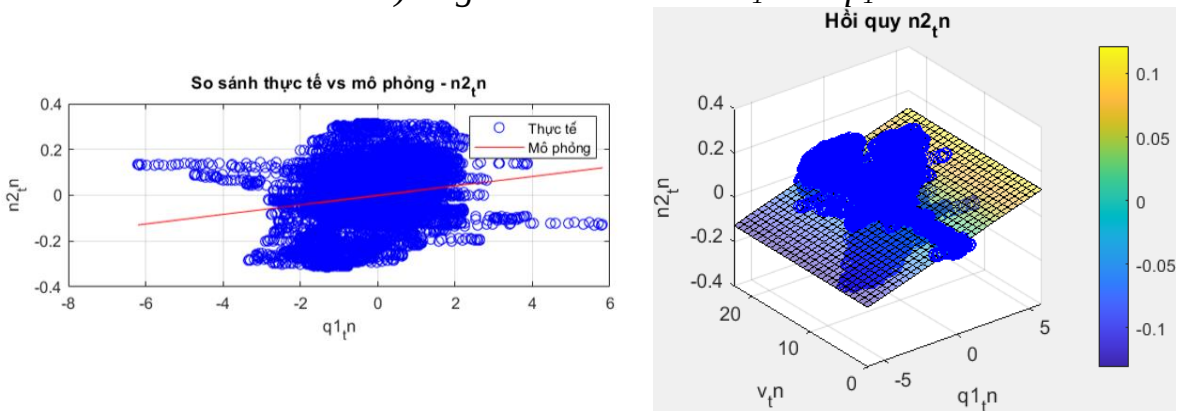

b) Regression between n_2 and q_1

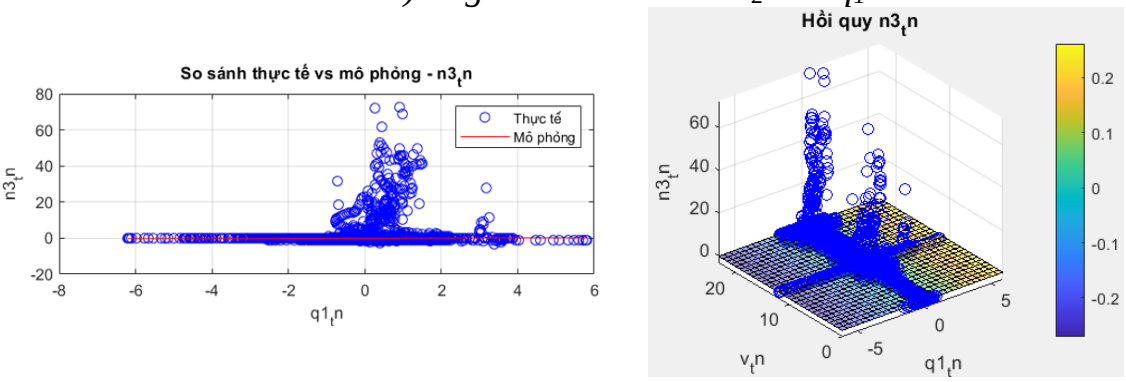

c) Regression between n_1 and q_1

Figure 4.31 Graph showing the effect of vehicle vibration on passenger vibration

The 2D plots on the left and the 3D plots on the right show that the regression plane always fits the actual experimental data, the vanishing points are located near the data plane, indicating that the regression model is suitable and does not require improvement for further experiments.

4.7.3 Evaluation of experimental result error

Plot the measurement results between q_{1_tn} and q_{1_mp} as shown in figure 4.32.

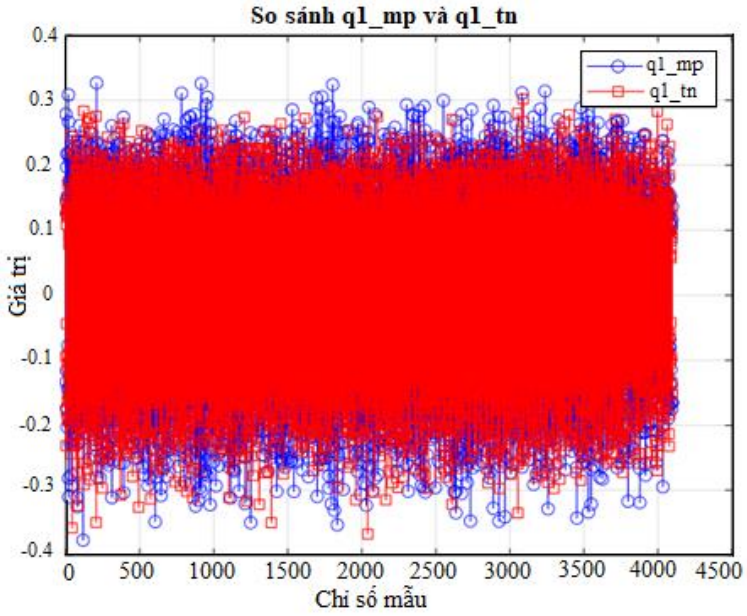

Figure 4.32 Graph of experimental results and simulation results of q_1

Thus, the difference between the simulation results and the experimental results is 11.3 (%) which is within the acceptable range.

4.8 CONCLUSION OF CHAPTER IV

Chapter IV establishes an experimental measurement procedure on the County 29-seat passenger bus and on seated occupants using a modern specialized measurement system (Dewesoft Sirius, ICP 356A16 accelerometers, and DS-IMU1 sensors). The application of a sensor misalignment angle correction method for sensors mounted on the human body, together with the use of a Butterworth filter, effectively removes measurement errors and signal noise, ensuring that the collected data shows good convergence with a coefficient of variation (CV) < 10%.

The experimental conditions were designed to be consistent with the simulation conditions. The actual road surface irregularities include sinusoidal bumps, impulse-type bumps, and random road profiles, with parameters equivalent to those used in the simulation model. The vehicle speeds in the experiments were lower than those used in the simulations, with V = 20, 40, and 60 km/h, because real-world conditions did not allow the test vehicle to operate at higher speeds of 80 and 100 km/h during the experiments.

Experimental results show that on random roads at speeds of 20, 40, 60 km/h, the oscillations are within the allowable limits. However, when the vehicle passes

through sinusoidal and pulse-shaped bumps, the oscillation acceleration at body positions increases sharply, especially at the thighs up to 5.1 m/s², causing extremely uncomfortable feelings for passengers, consistent with theoretical observations.

Correlation and regression analysis showed that the variation laws of experimental and simulated data were consistent. The average percentage error between the simulated and experimental acceleration values was **11.3%**, indicating that the experimental model was reliable.

GENERAL CONCLUSION AND FURTHER RESEARCH DIRECTIONS OF THE THESIS

GENERAL CONCLUSION

The overview study has provided assessments on the importance and necessity of the issue of car vibration for the quality of the car in use through the health standards of the occupants . The thesis has taken the vibration acceleration index in the international standard ISO 2361-1 to evaluate the impact of car vibration on the occupants.

The thesis has built a space model and oscillation equations of a 9-degree-of-freedom vehicle, including 7 degrees of freedom of the vehicle and 2 degrees of freedom of two vertical seat positions including the passenger seat and the third row seat.

Build and solve the 3-mass model of a person sitting on a chair using a 3-degree-of-freedom mass-spring model, including head mass, chest mass and thigh mass, in which the thigh mass represents the back, torso, arms, legs and buttocks of a person.

Using the finite element method to simulate 3D chair-human model, the reliability on the head of the two methods has $R^2 = 0.7311/0.692$, on the chest has $R^2 = 0.7513/0.6334$, on the thigh there is $R^2 = 0.8015/0.2972$ which helps increase the reliability of simulation results in Matlab/Simulink when only considering vertical vibrations .

Experimental results show that on random roads at speeds of 40 and 60 km/h, the oscillations are within the allowable limits. However, when the vehicle passes through sinusoidal and pulse-like bumps, the oscillation acceleration at body positions increases sharply, especially at the thighs up to 5.1 m/s², causing

extremely uncomfortable feelings for passengers, consistent with theoretical observations.

Correlation and regression analysis showed that the variation laws of experimental and simulated data were consistent. The average percentage error between the simulated and experimental acceleration values was 11.3% , indicating that the experimental model was reliable. The results obtained surveys provide a scientific basis for proposing improvements to passenger bus seats manufactured and assembled in Vietnam.

DIRECTIONS FOR FURTHER RESEARCH

Due to some objective and subjective reasons, the topic still has some limitations that need further research expansion:

1. Continue to survey the vibration of all seat positions in the car, create an vibration diagram of the entire car floor.

2. Continue to examine the vibration of the entire human body.

3. Comparison of the complete set of simulation results and experimental results

4. Optimize the seat structure to suit the vehicle floor vibration positions.

LIST OF PUBLISHED SCIENTIFIC WORKS

[1]. *Le Duy Long, Nguyen Thanh Quang* , Study on bus noise and vibration with selected material , 2023 3rd International Conference on Electrical, Computer, Communications and Mechatronics Engineering (ICECCME), Tenerife, Canary Islands, Spain, 2023, pp. 1-4.

[2]. *Le Duy Long, Nguyen Thanh Quang, Le Hong Quan, Phi Hoang Trinh, Le Duc Hieu* , Effect of road surface on vibration of passengers in s , HaUI Journal of Science and Technology, Vol. 60 - No. 5 pp. 209 -212, May 2024.

[3]. *Le Duy Long, Nguyen Thanh Quang, Le Hong Quan, Pham Minh Hieu, Le Duc Hieu* , Analysis of vibration experienced by passengers and their seats in a , HaUI Journal of Science and Technology, Vol. 60 - No. 5 , pp. 219 -221, May 2024

[4]. *Le Duy Long, Nguyen Thanh Quang, Le Hong Quan, Nguyen Xuan Khoa, Tran Huy Hoang, Le Dinh Dat, Tran Duc Binh* , Simulation study of vibration of 5-seat sedan **,** HaUI Journal of Science and Technology, Vol. 61 - No. 7E , pp. 95 - 98, July 2025.

[5]. *Le Duy Long, Nguyen Thanh Quang, Le Hong Quan, Nguyen Xuan Khoa, Nguyen Viet Hoa, Le Dinh Dat, Tran Duc Binh* , Simulation study of vibration of 5-seat sedan **,** HaUI Journal of Science and Technology, Vol. 61 - No. 7E , pp. 115 - 118, July 2025.

[6]. *Le Duy Long, Nguyen Thanh Quang, Le Hong Quan, Tran Duc Binh , Nguyen Thai Van,* Experimental Study on the Effect of Vehicle Vibrations on Passengers in a 29-Seat Coach**,** The International Conference on Machines, Energy and Digitization for Sustainable Development (IMEDS 2025) 2025, September Vinh Long Province, Vietnam.